SIZING STUDIES OF LIGHT AIRCRAFT WITH SERIAL HYBRID PROPULSION SYSTEMS

J. Ludowicy, R. Rings, D. F. Finger, C. Braun
FH-Aachen, Institute of Aircraft Engineering
Hohenstaufenallee 6, 52064 Aachen, Germany

Abstract

In this paper, the viability of general aviation aircraft with serial hybrid-electric powertrains is examined. They will be compared to conventionally powered aircraft with similar specifications, by the means of initial sizing results. Studies on battery specific energy and aerodynamic efficiency will be analyzed, the latter in the scope of a distributed electric propulsion concept, to see their influence on the viability of serial hybrid aircraft. Results show that a serial hybrid-electric aircraft with an optimized distributed electric propulsion concept is competitive to today's conventionally powered light general aviation aircraft, while enabling significant fuel savings.
Additionally parameter variation studies are conducted to see the influence of take-off distance, aircraft range and cruise speed on the optimal design point. The finding is that the conventional design rule is not valid anymore and for every new hybrid-electric aircraft a design space exploration should be conducted.

NOMENCLATURE

BSFC	=	Brake Specific Fuel Consumption
Bat	=	Battery
CTOL	=	Conventional Take-off and Landing
c_D	=	Drag Coefficient
conv	=	Conventional
DoH	=	Degree of Hybridization
E	=	Energy
E^*	=	Specific Energy Density
EM	=	Electric Motor
GA	=	General Aviation
g	=	Gravitational Acceleration
H_E	=	Degree of Hybridization of Energy
H_P	=	Degree of Hybridization of Power
h	=	Height
ICE	=	Internal Combustion Engine
L/D	=	Lift-to-Drag Ratio
m	=	Mass
MSL	=	Mean Sea-Level
MTOM	=	Maximum Take-off Mass
nd	=	Not Defined
P	=	Power
P/W	=	Power-to-Weight Ratio
PE	=	Primary Energy
RE	=	Range Extender
S	=	Wing Area
Spec	=	Specific
T/W	=	Thrust-to-Weight Ratio
TOD	=	Take-off Distance
t	=	Time
VTOL	=	Vertical Take-off and Landing
v	=	Velocity
W/S	=	Wing Loading
η	=	Efficiency
μ	=	Ground Friction Coefficient

1. INTRODUCTION

Environmental awareness increased steadily over the past decades and climate change has become an omnipresent topic. As one result, aviation is facing new challenges concerning less emissions and less consumption of fossil fuel for new aircraft. The goals are e.g. defined by *Flightpath 2050* published by the European Commission, which demands a decrease of CO2 emissions for new aircraft in the year 2050 of 75 % and 90 % in NOx in comparison to new aircrafts from the year 2000 [1].
These targets will most likely not be met by just improving today's technology, but rather call for new aircraft concepts. Electric propulsion is a promising field of technology by which such reductions could be achieved. Unfortunately, the technology is not yet ready for fully electric propulsion in a broad application range. The energy density of batteries is still the limiting factor as it is multiple times lower than for fossil fuel (e.g. [2] [3]). The medium-term solution is likely the hybrid-electric powertrain. In a serial hybrid configuration, superior efficiency [4] and higher specific power [5] of electric motors make the use of concepts like Distributed Electric Propulsion (DEP) [6] possible, while internal combustion engines can use the high specific energy of fossil fuel. The combination of both propulsion methods as a serial hybrid offers new degrees of design freedom but has to be optimized to utilize its full potential.

While hybrid-electric transport aircraft have been studied in depth (e.g. [7], [8] or [9]), research is still lacking on the topic of General Aviation (GA). This paper aims to answer the question under which conditions light GA aircraft with serial hybrid-electric powertrains utilizing today's technology are competitive to conventionally powered aircraft.
The primary assessment criterion is maximum take-off mass (MTOM). Additionally primary energy and fuel usage will be assessed.
A conventional baseline aircraft will be sized first and then a serial hybrid-electric aircraft without any integration benefits will be compared, as well as an aircraft that includes a DEP concept.

doi:10.25967/480226

Furthermore a study on the battery energy density is conducted, to see the influence on the MTOM as well as energy and fuel usage.
Additionally, parameter variations on important aircraft specifications are analyzed on their influence on the optimal design point (DP), best Degrees of Hybridization, MTOM and viability against conventional aircraft. As the conventional rule for choosing the design point seems to be not valid for hybrid aircraft anymore, it will be checked if a new rule for these aircraft can be established. The parameters that will be investigated are take-off distance (TOD), range and cruise velocity.

This paper is structured the following way: Following this introduction, the used initial sizing methodology is briefly presented in chapter 2. Then, in section 3, the conventional baseline aircraft will be defined and compared to a serial hybrid. In chapter 4 the parameter variations are conducted. The DEP concept and integration benefits will be applied to the sizing of an improved serial hybrid in chapter 5. Finally, chapter 6 gives a comprehensive conclusion.

2. METHODOLOGY

The results that are shown and discussed in chapters 3 and 4 and 5 were produced using an initial sizing tool that was developed at FH Aachen. It was already used for sizing studies on CTOL and VTOL aircraft in [10] and [11]. The methodology implemented in this tool is described in detail in [12]. However, the core elements of the method will be briefly presented in this chapter, as this will help to understand the most important differences between a conventional sizing approach and the new sizing methodology for hybrid electric aircraft.

The sizing algorithm is separated into two major parts – Point Performance and Mission Performance – and hence, is similar to classical sizing approaches.
For both parts it is necessary to insert certain input parameters. These specify the flight mission, the aerodynamics and the propulsion system. This includes the type of powertrain, while there are four possibilities of propulsion systems in this methodology:

- The conventional powertrain, as used in the majority of today's GA aircraft, where an internal combustion engine (ICE) is mechanically connected to a propeller, optionally via a gearbox.

- The fully electric powertrain, where an electric motor (EM) with power supply from batteries drives the propeller. It is the counterpart of the conventional powertrain.

Between those two kinds of powertrains which represent the extremums of the powertrain spectrum, there are the partially electrified hybrid powertrains. The types of hybrid powertrains commonly used are the parallel and the serial hybrid setup (see Figure 1).

- For the serial hybrid powertrain, the propeller is solely driven by an EM, which is sized according to all performance requirements. A multiple propeller layout, where each propeller has its own EM, is also possible. The electric power for the EM is provided either by batteries or a fuel burning ICE driving a generator. The ICE and generator are usually called Range Extender.

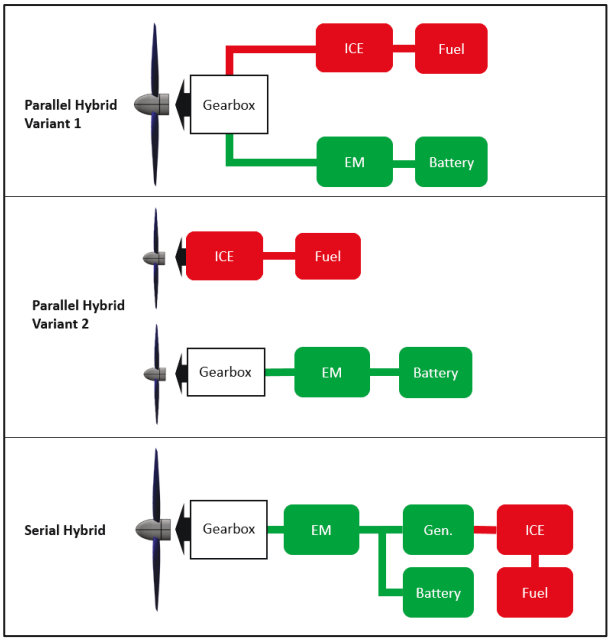

Figure 1 – Types of Hybrid Powertrains

- For the parallel hybrid powertrain, an EM and an ICE are both mechanically connected to a propeller shaft, often via a gearbox when both are connected to the same propeller shaft (Variant 1). Alternatively EM and ICE each drive one propeller, which is also considered a parallel hybrid (Variant 2). Just as for the serial hybrid case, designs with multiple propulsion units for one aircraft are possible.

Once all inputs regarding the mission, the aerodynamics and the propulsion system are defined, the search for the optimal design point with its values for thrust-to-weight ratio (T/W), respectively power-to-weight ratio (P/W) and wing loading (W/S) as well as the connected Degree of Hybridization (DoH) starts. For that purpose, a constraint diagram is generated. It considers the constraints presented by Gudmundsson [13], in a slightly modified form (see [12]). Those constraints are for example the desired rate of climb, the desired take-off distance or the desired cruise airspeed. Next, the whole design space of this constraint diagram is discretized by points in a pattern. Each point represents a different combination of T/W or P/W and W/S and Degrees of Hybridization of H_P and H_E. Every point is then analyzed using the Mission Performance part of this sizing algorithm. Afterwards the results are scanned for the optimal point that provided the best results concerning the design objective, in this case lowest MTOM.

2.1. Degree of Hybridization of Power

In this context H_P is the DoH of Power, which is the ratio of the installed propulsion power of all electric motors to the total installed propulsion power at the propeller shaft(s) (see Equation 1).

$$(1) \quad H_P = \frac{P_{EM,max}}{P_{max}}$$

It is defined once for every aircraft and its propulsion system configuration. For the sizing process, the H_P values are determined by the ratio of the power demand at the current split point inside the constraint diagram to the overall power

demand arising from the current design point (Figure 2).
Note that for serial hybrid-electric powertrains, the DoH of Power H_P, as it is defined above, is always one, since the EM must be able to solely deliver the total needed power. To differentiate between the all-electric powertrain and to size the Range Extender, an additional DoH of Power for serial hybrids is introduced by Equation 2.

(2) $H_{P.serial} = \frac{P_{EM,max}}{P_{ICE,max}}$

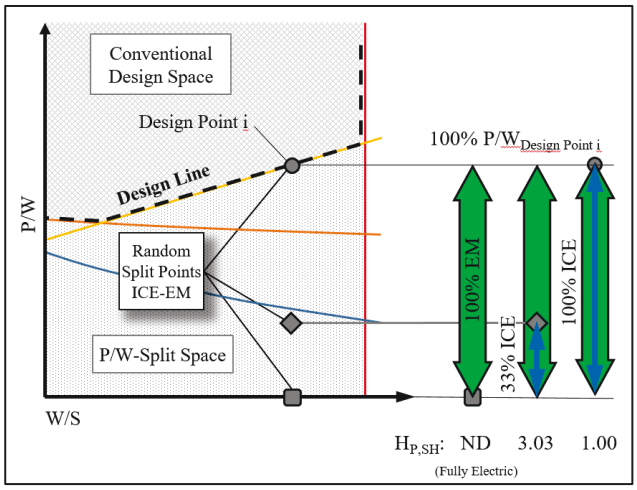

Figure 2 – Hybridization inside the Constraint Diagram

2.2. Degree of Hybridization of Energy

The parameter H_E is the DoH of Energy, which is specified as the ratio of the in-flight required transport energy delivered by batteries ('non-consumable', as the batteries do not lose weight while being discharged) to the total required transport energy (see Equation 3). It is defined for every flight phase of a mission (labeled as 'i') and determines the power request of EM and ICE in every moment of each phase.

(3) $H_{E,i} = \frac{\Delta E_{non-consumable}}{\Delta E\_total}$

For the sizing process, the different values for H_E for every flight phase are determined by the ratio of the power requirement of the electric motor in the considered phase to the total power demand of the phase, which is represented by its constraint (see Figure 2). That means, e.g. that the H_E of a phase is zero if the split point is located above the relevant constraint. It is bigger than zero if the ICE is not able to generate the totally needed power, which would be the case if the split point is located underneath the constraint.
For the sizing the values of T/W or P/W and W/S are, contrary to the Degrees of Hybridization, for whose definition the split point is crucial, solely defined by the design point during the Point Performance calculations (see Figure 2). That means there are multiple points which share W/S and P/W but the Degrees of Hybridization H_P and H_E are different for each split point.

2.3. Transport Energy Calculation

In the mission performance part, the actual sizing of the aircraft and its components takes place as an iterative process to determine the key parameter MTOM. During the iteration, the whole mission is simulated, while it is divided into multiple time steps.
First, an initial value for the MTOM has to be assumed. Then, according to the T/W or P/W, the installed thrust, respectively power is calculated, also taking into account the DoH of power to distribute the maximum power to EM and ICE. Using this information, the propulsion system is sized, as its engine-, motor- and integration masses are computed. Besides, the wings are sized by their reference area S, using the wing loading W/S.
To calculate the energy carrier masses the needed transport energy during the whole mission has to be calculated. This is done by determining the required energy in every time step of a flight phase, considering all energy requirements which may occur in this phase. Energy demands can arise from the compensation of aerodynamic drag, acceleration (kinetic energy), altitude change (potential energy) and ground friction. Equation 4 gives the total needed transport energy in every time step of a mission phase, while the individual energy demands are presented thereafter. For particular phases, some energy demands may not occur and therefore be zero (e.g. ground friction for cruise flight). Note that the energy in take-off results from the operation of the powertrain at the maximum thrust or power for a specified time.

(4) $\Delta E = \Delta E_{drag} + \Delta E_{acc} + \Delta E_{alt} + \Delta E_{gf}$

with

(5) $\Delta E_{drag} = m * g * v * \frac{D}{L} * \Delta t$

(6) $\Delta E_{acc} = \frac{1}{2} * m * (\Delta v)^2$

(7) $\Delta E_{alt} = m * g * \Delta h$

(8) $\Delta E_{gf} = \mu * m * g * v * \Delta t$

If power specific propulsion devices like the ICE and the EM are regarded, the transport energy is divided into consumable energy (fuel) and non-consumable energy (from batteries) by the DoH of Energy given in Equation 3. For thrust specific devices like the jet engine, the transport energy is not split, since the hybridization of propulsion systems including jet propulsion is not included in this methodology.
After the energy distribution, the power in a time step of a mission phase is computed for each ICE and EM using Equations 9 and 10. In this context, it is essential to respect an efficiency from shaft to thrust for power specific propulsion devices [12].

(9) $P_{ICE} = \frac{\Delta E_{consumable}}{\eta * \Delta t * n}$

(10) $P_{EM} = \frac{\Delta E_{non-consumable}}{\eta * \Delta t * n}$

For combustion engines it is necessary to compare the required power with the maximum power that can be delivered by the propulsion device at the current altitude, which is done via a models from [14].
Before the resulting energy carrier masses of battery and fuel can be calculated, which are needed in a time step of a mission phase, it is assessed whether a recharging of batteries by an ICE is possible and desired. This is, amongst others, dependent on the power rating of each ICE, as an ICE running at maximum power loading to fulfill the mission requirements cannot deliver additional power for recharging.

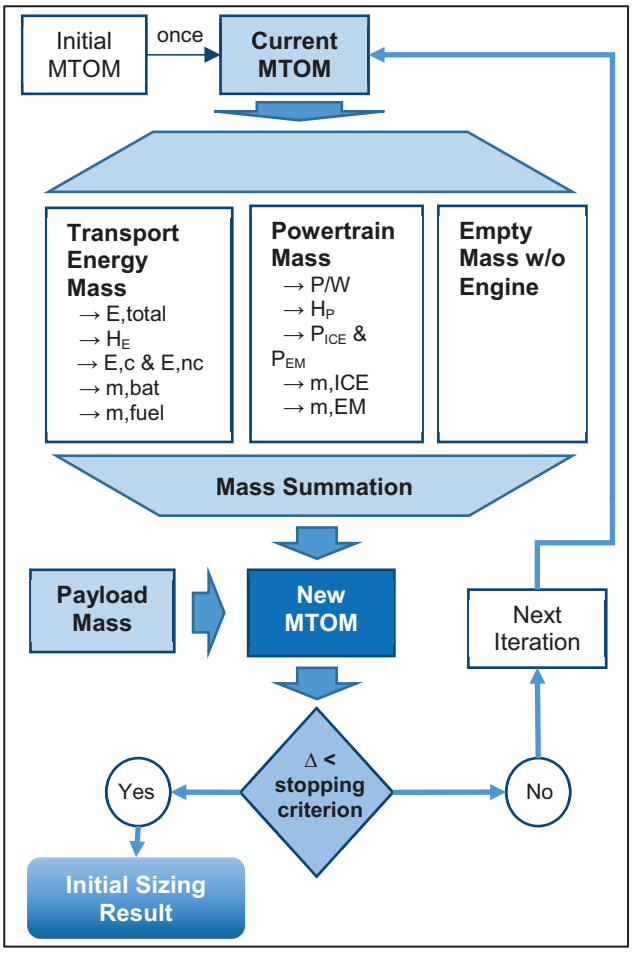

Figure 3 – MTOM Iteration Cycle

2.4. Mass Estimation

The calculation of the energy carrier masses, which is performed in each time step to successively sum up these masses to the total required energy carrier masses for a whole mission, is described in Equations 11 and 12.

$$(11)\ \Delta m_{fuel} = P_{ICE} * n * BSFC * \Delta t$$

$$(12)\ \Delta m_{battery} = \frac{\Delta E_{non-consumable}}{\eta * \rho}$$

As can be seen, for fossil fuels, this calculation requires additional information about a specific fuel consumption (SFC) of the engine. Therefore a model is implemented that correlates current power output or thrust with a SFC. Information about an efficiency of the conversion from energy in the batteries to thrust, the included propeller efficiency as well as a battery energy density are essential for the calculation of the battery weight. Hence models to estimate these values are also included.

To respect the weight loss of an aircraft, which is fully or partially powered by fuel burning engines, and the consequences on the overall transport energy demand, the fuel mass computed in every time step is subtracted from the current mass of the aircraft.
In a final step, the determination of an empty mass fraction without dry engine mass and without engine integration masses is essential to sum up all the calculated masses to the new MTOM and to provide a mass breakdown of the sized aircraft (see Equation 13). This empty mass fraction without engine (emfwe) is derived from statistical data dependent on the MTOM of the aircraft.

$$(13)\ MTOM = m_{emfwe} + m_{energy} + m_{drive\ train} + m_{payload}$$

Based on the new MTOM, the next iteration step can be started. The iteration stops, when the new calculated MTOM differs less than a defined stopping criterion from the one of the last iteration step. The whole weight iteration cycle is depicted in Figure 3.
As a second figure of merit besides the MTOM, the consumption of primary energy for every sized aircraft is calculated. The primary energy is a measure for total energy that was harvested directly from natural resources to provide an amount of energy to the consumer. Fuel for example has to be refined from raw oil, which prior had to be extracted from the soil. All of this used energy to produce the fuel is summed up in the primary energy factor (PEF). The factors in Germany from 2016 are 1.1 for fossil carbon based fuel and 2.8 for electricity [15]. The factor for electricity is that high because of the current composition of electricity where coal-burning and nuclear power plants have a big share, which have a high PEF. The factor will decrease as the use of renewable energy sources increases.

3. VIABILITY ASSESSMENT

In this section, the methodology described above is applied to study the viability of serial hybrid electric aircraft with today's technology in comparison to conventionally powered aircraft.

3.1. Baseline Aircraft

To make assumptions about the viability of serial hybrid-electric aircraft a reference has to be defined. The aircraft that will be used for this reason is a generic single-engine, unpressurized GA aircraft that was also sized with the aforementioned methodology. The top level requirements, mission specifications and technology assumptions are gathered in Table 1. The aircraft is roughly comparable to a Cessna 172 from its specifications [16]. The same baseline aircraft is used in [17].

These input parameters lead to the constraint diagram that can be seen in Figure 6. The decisive constraints are turn and take-off distance. Inside the figure the conventional DP is marked with a red circle.
The sizing calculation shows, that the conventional DP amongst all design points that represent conventionally powered aircraft (H_P = 0) yields the lightest aircraft that fulfills all of the requirements. The MTOM and consumption of primary energy as well as a mass breakdown can be found in Table 2.

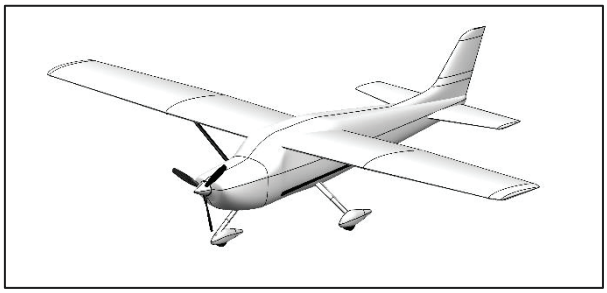

Figure 4 – Impression of Baseline Aircraft

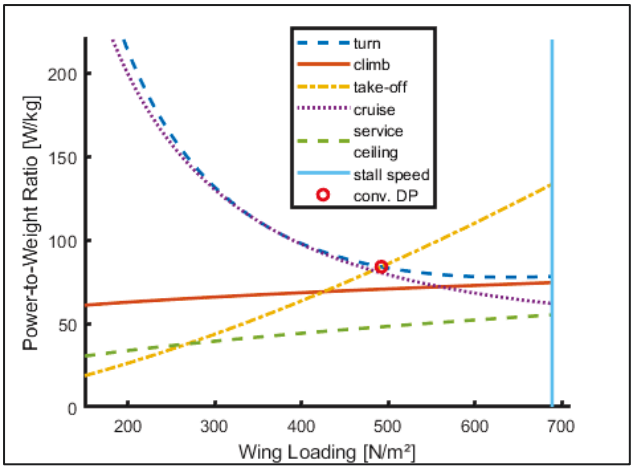

Figure 6 – Constraint Diagram Baseline Aircraft

Table 1 – Parameters Baseline Aircraft

Requirements	
Take-off Ground Roll [m]	200
Rate of Climb at MSL [m/s]	4
Stall Speed [m/s]	25
Cruise Speed [m/s]	55
Payload [kg]	300
Mission	
Taxi & Take-off	at MSL
Climb	to 2500m
Cruise	for 1000km
Loiter	for 45 min
Descend, Landing, Taxi	MSL
Technology	
ICE Spec. Power [kW/kg]	1
EM Spec. Power [kW/kg]	5
SFC_{ICE} [kg/kW/h]	0.35
Bat. Energy Density [Wh/kg]	250
C_{D0} [counts]	300
Induced Drag Factor k [-]	0.0566
$C_{L,max}$ [-]	1.8
$C_{L,TO}$ [-]	1.2

Table 2 – Results Baseline Aircraft

Conventional Baseline Aircraft	W/S [N/m²]	P/W [W/kg]	MTOM [kg]	Primary E. [GJ]
	492	84	1090	6.76

Mass breakdown, all values in [kg]

Empty mass (w/o engine)	ICE mass	Fuel mass	EM mass	Battery mass
532	115	143	0	0

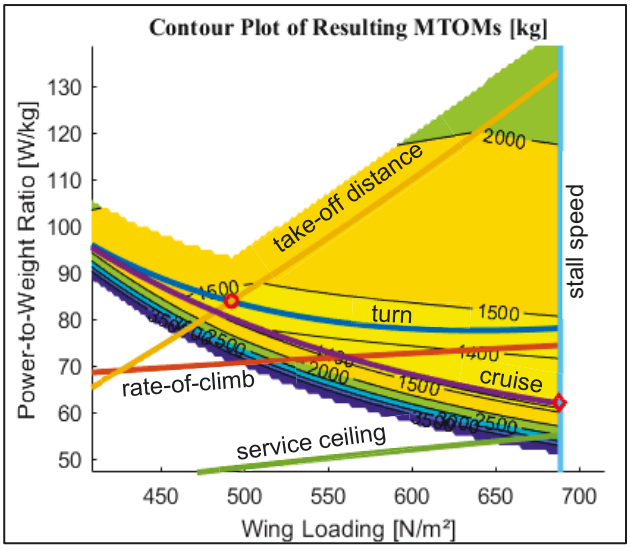

Figure 5 – Constraint Diagram including MTOM Contour Plot for the Serial Hybrid

3.2. Serial Hybrid Aircraft

The same requirements, mission and technology assumptions (see Table 1) are used to size a serial hybrid-electric aircraft. The contour plot of the resulting MTOMs for all split points can be seen in Figure 5. From its structure the plot is similar to Torenbeeks thumbprint plots for conventional aircraft [18].

The first thing that can be observed from this MTOM contour plot is that the cruise constraint has a strong influence on the overall weight. For split points below this constraint, the MTOM drastically increases until it exceeds 5670 kg for which the results are not of interest for GA aircraft anymore and therefore not included. On the other hand, the lightest aircraft with a serial hybrid-electric powertrain, marked by the red diamond, is just above the cruise constraint. An aircraft at that split point has an ICE that is sized for the cruise requirement, meaning it runs at full power during cruise and therefore at peak efficiency, following the used SFC model. The EM is sized to meet all power requirements, in this case roughly 170 kW. The batteries provide extra power for the mission phases with a higher power demand than cruise like take-off or climb.

The MTOM of this lightest serial hybrid solution is 1300 kg, which is an increase of ca. 20 % in comparison to the conventionally powered baseline aircraft. Also considering primary energy use it is inferior as it would use ca. 7 % more.

The more interesting finding is that this result is not achieved at the conventional DP. The design and split point are located at the maximum wing loading. To see how different parameters influence the location of the design point, the parameter variation studies in chapter 4 are conducted.

A detailed mass breakdown of this serial hybrid aircraft can be found in Table 3. It shows for example that the Range extender unit, which is sized to only 63 W/kg as can be seen in Figure 5, is heavier than the ICE sized to 84 W/kg for the conventionally powered aircraft, because it includes an additional generator and suffers from additional conversion losses, which contributes to the overall heavier weight. Further, no fuel could be saved, instead the fuel mass increased slightly. Additional 50 kg of battery mass are

needed. All of this leads to an overall heavier aircraft which is not competitive to a conventionally powered aircraft. The H_P of this aircraft would be 1 and the $H_{p,serial}$ would be roughly 2.1, meaning, the ICE is sized to produce less than one third of the power of the EM.

Table 3 – Results Serial Hybrid-Electric Aircraft

Serial Hybrid-Electric	W/S [N/m²]	P/W [W/kg]	MTOM [kg]	Primary E. [GJ]
	680	132	1300	7.24
Δ to conv.	+38%	+57%	+19%	+7%

Mass breakdown, all values in [kg]

	Empty mass (w/o engine)	RE mass	Fuel mass	EM mass	Battery mass
	629	138	149	34	50
Δ	+18%	nd	+4%	nd	nd

4. PARAMETER VARIATIONS

As stated before, the following parameter studies are conducted to analyze the influence of take-off distance, range and cruise velocity on the design point. The one parameter that is currently analyzed will be changed while all other values will be kept at the values from Table 1.

4.1. Take-off Distance Variation

The take-off distance changed from 100 up to 999 meters. The results, listed in Table 4, show no influence of the take-off distance on the design point. For every value, the design point is located at the maximum wing loading of 688 N/m² and the split point always right above the cruise constraint. The overall P/W ratios and the $H_{P,serial}$ decreases until a TOD of 600m. For these very high distances the take-off constraint is not decisive for the overall P/W anymore and therefore the results do not change.
As described in section 2.1, the $H_{P,serial}$ in combination with the overall P/W describes the part of the power that is delivered by the ICE which is later translated into the size of the ICE. This portion stays constant for all take-off distances, at 62 W/kg, meaning the split point is always just above the cruise constraint. Meanwhile, the share of the EM increases and therefore it gets heavier for decreasing take-off distances. At the same time the weight of all other components is also increased by the avalanche effect which is typical for initial sizing.
Even for the lowest value for the take-off distance of only 100m with a P/W of ca. 250 W/kg, where the conventional point would only need a P/W of about 110, as can be seen in Figure 7, the lowest MTOM was achieved at the maximum wing loading. That shows that the benefit from a smaller wing during cruise, at least up to this value for the take-off distance, is higher than the benefit of needing less than half the overall installed power.

For the increasing take-off distances the MTOM decreases, as can be seen in Figure 8. But even for the highest TOD, the serial hybrid aircraft with 1177 kg is still heavier than the conventional aircraft with its 1090 kg. The red line in Figure 8 shows the resulting MTOMs for a parameter variation of TOD for a conventional aircraft. For no TOD in the investigated range the serial hybrid is lighter.

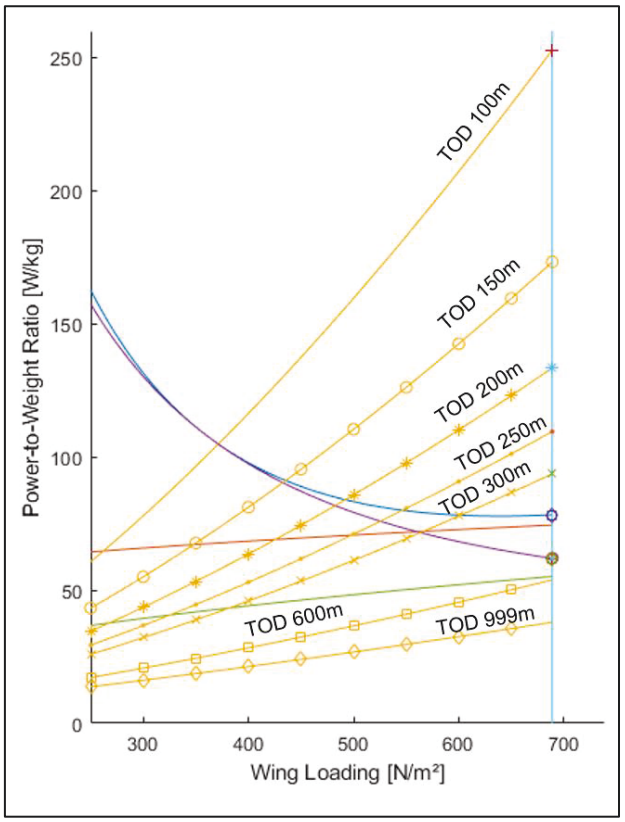

Figure 7 – Constraint Diagram TOD Variation

Table 4 – Results Take-off Distance Variation

TOD [m]	W/S [N/m²]	P/W [W/kg]	$H_{P,serial}$ [-]	MTOM [kg]	PE [MJ]
100	688	253	4.08	1485	8140
150	688	173	2.79	1363	7496
200	688	133	2.15	1300	7175
250	688	110	1.77	1256	6967
300	688	94	1.51	1221	6806
600	688	78	1.26	1177	6614
999	688	78	1.26	1177	6614

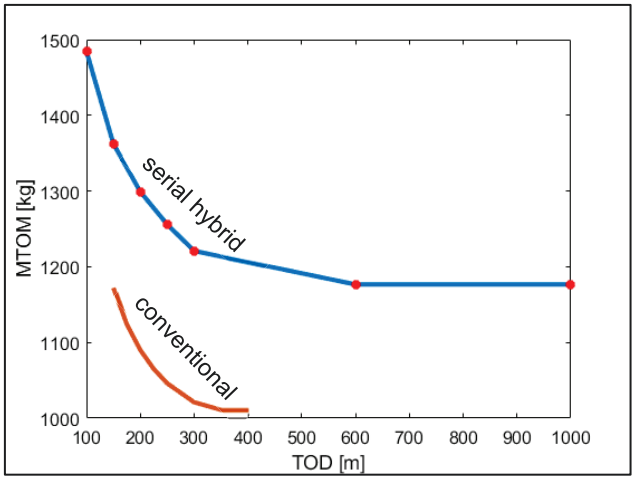

Figure 8 – MTOM over Take-off Distance

4.2. Range Variation

The range is a parameter that does not affect the constraints of the constraint diagram, but was identified as crucial, as it defines the length of the cruise segment. As this is the segment where the hybrid with a higher wing loading gains most of its benefits, a study is conducted. Different ranges from 100 up to 3000 km are analyzed.

The results are presented in Table 5. They show that there is an influence of the range on the design point.
For low ranges up to 310 km the lowest MTOM was achieved with approximately the wing loading of the conventional design point of 494 N/m². From 320 up to 3000 km the design point was constantly located at the highest possible wing loading of 688 N/m². Simultaneously the P/W and $H_{P,serial}$ changed, but were also constant before and after. Again the split point was always located right above the cruise constraint, independent of the range.
For low ranges, the fuel savings of an ICE, running at best fuel economy and being smaller and thereby lighter than for the conventional powertrain, are not as big as for longer ranges. That makes the additional EM and batteries not feasible as they would increase the overall mass. At one point the savings are big enough to carry the additional mass and still being lighter than the configuration from the conventional DP, in this case at a range between 310 and 320 km.
For this resolution of the search pattern and chosen ranges it appears that the design point jumps suddenly, while in reality it is more likely that it increases with a few steps in between up to the maximum wing loading.

The resulting MTOMs increase steadily with increasing range. The correlation can be seen in Figure 9. Again, the results for a similar variation for a conventional aircraft are added and show, that for none of the investigated ranges the serial hybrid is lighter.
The increase in MTOM is exponential as the mentioned avalanche effect increases the total weight if more fuel mass is needed. The used primary energy shows the same trend of exponential increase.
A serial hybrid aircraft with an equal MTOM to the conventional baseline aircraft would only be able to fly about 500 km, which is a loss of half of its range.

Table 5 – Results Range Variation

Range [km]	W/S [N/m²]	P/W [W/kg]	$H_{P,serial}$ [-]	MTOM [kg]	PE [MJ]
100	494	84	1.06	945	1425
200	494	84	1.06	981	2085
300	494	84	1.06	1021	2798
310	494	84	1.06	1025	2873
320	688	133	2.15	1028	2384
400	688	133	2.15	1055	2844
500	688	133	2.15	1089	3452
1000	688	133	2.15	1299	7175
1500	688	133	2.15	1599	12564
2000	688	133	2.15	2057	20940
2500	688	133	2.15	2823	35251
3000	688	133	2.15	4326	63986

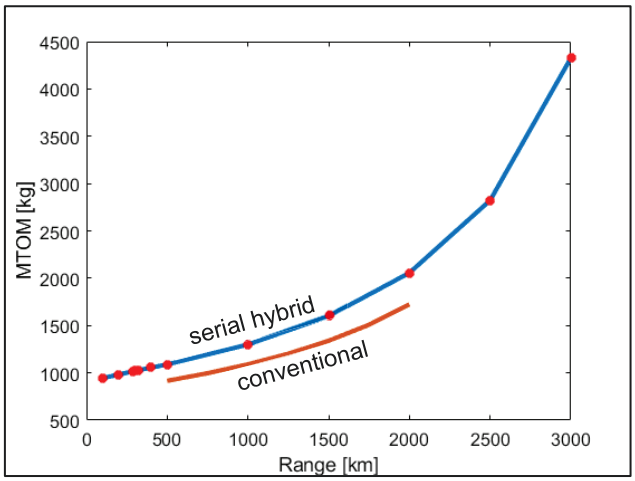

Figure 9 – MTOM over Range

4.3. Cruise Velocity Variation

The cruise velocity has a direct influence on the cruise and turn constraint in the constraint diagram. Therefore a parameter variation for values from 40 to 75 m/s is conducted.

From the data in Table 6 as well as from Figure 10 it is clearly visible that the cruise velocity has an influence on the design point. For a cruise velocity of 40 m/s the constraint is not decisive as other constraints are always higher. But, for the first time, the design point is not located in the conventional point or at the maximum wing loading. It is at a slightly higher wing loading and P/W. The split point is still right above the cruise constraint. For 45 m/s cruise velocity the cruise and turn constraint are only relevant for very low wing loadings. Again the design point is in between the conventional and maximum wing loading, roughly in the middle between those two. As can be seen in Figure 10, the slope and the height (power demand) of the cruise constraint over the given range of wing loadings increases with higher cruise velocities. This is the reason why the best wing loading changes. For the first two velocities, the slope of the cruise constraint is too low so that the additional fuel and ICE mass savings for split points at higher wing loadings in comparison to the chosen design point are not high enough to make up for the additional weight of a bigger EM and battery that would be required because of the strongly increasing take-off distance constraint.
For cruise velocities from 50 up to 75 m/s the best design point seems to be at the maximum wing loading, but due to the finite resolution they fluctuate between wing loadings of 672 and 688 N/m².
The cruise velocity of 75 m/s results in a configuration with nearly no batteries, as the whole power is delivered by the ICE, as the $H_{P,serial}$ is approximately one.

The MTOM increases again exponentially over increasing cruise velocity, as can be seen in Figure 11. The trend for the primary energy is also again an exponential increase.
A serial hybrid aircraft with the same MTOM as the conventional baseline aircraft would only be able to fly at about 43 m/s, over the whole cruise distance of 1000 km that would be a time penalty of approximately 80 minutes. The resulting MTOMs from the same parameter variation for conventional aircraft are added as the red line in Figure

11. It can be seen, that for all velocities except 40 m/s, the serial hybrid aircraft is heavier. For low cruise velocities the MTOMs seem to converge, but only due to bad choices of the conventional design point of the algorithm [19].

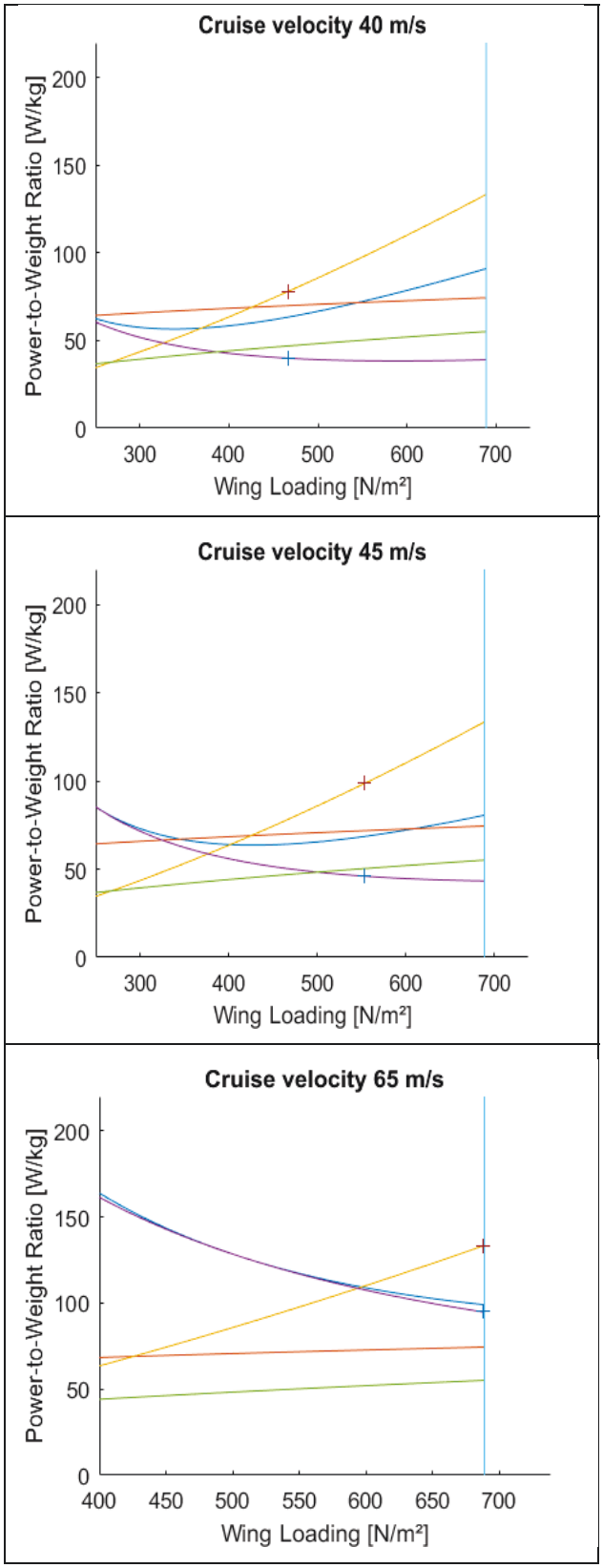

Figure 10 – Example Constraint Diagrams for Cruise Velocity Variation

Table 6 – Results Cruise Velocity Variation

Cruise v [m/s]	W/S [N/m²]	P/W [W/kg]	$H_{P,serial}$ [-]	MTOM [kg]	PE [MJ]
40	466	78	1.95	1050	5138
45	554	99	2.15	1113	5569
50	688	133	2.61	1187	5949
55	672	129	2.05	1305	7313
60	684	132	1.72	1485	9274
65	688	133	1.40	1788	12618
70	688	133	1.14	2333	18704
75	688	143	1.00	3858	35048

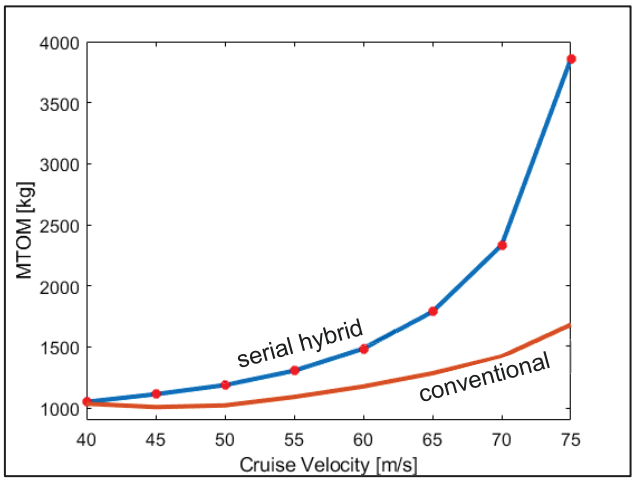

Figure 11 – MTOM over Cruise Velocity

5. SERIAL HYBRID AIRCRAFTS WITH INTEGRATION BENEFITS

As seen in chapters 3 and 4, a serial hybrid-electric aircraft without any integration benefits or without relaxing the requirements or modifying the mission is heavier and consumes more fuel.

In the following, such integration benefits are considered, for example a distributed electric propulsion concept.

Such a DEP concept, like the one the NASA intends to use for the X-57 plane [20], where multiple small electric motors are distributed over the whole wingspan to accelerate the local flow over the wing, can increase the maximum lift coefficient of an aircraft significantly [21] [22]. The maximum lift coefficient for the next calculation was set to 4, to account for such a DEP concept. For the take-off a lift coefficient of 2 was assumed. The original values of the baseline aircraft were 1.8 as maximum and 1.2 for take-off, as can be seen in Table 1. What is not accounted for in this calculation, is the energy as fuel or in battery mass to power the multiple electric motors to achieve the higher lift coefficients during take-off and landing.

This is going to affect the stall speed constraint, which will open the design space to much higher wing loadings, and the take-off distance constraint, which will be significantly lowered. For comparison, the old constraints for stall speed and take-off distance are added as dashed lines.

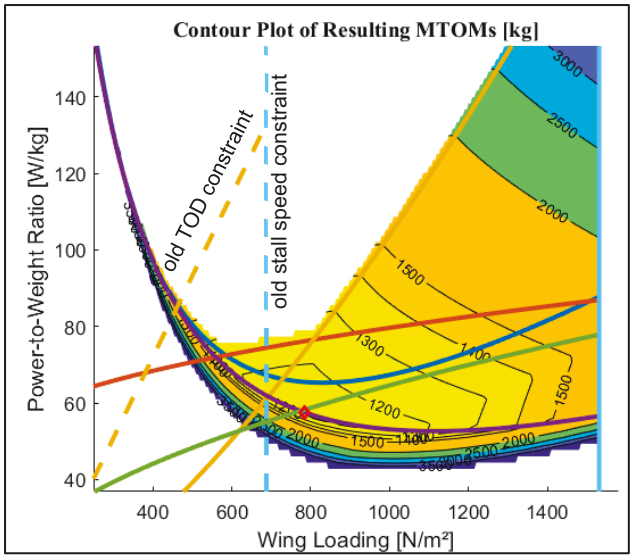

Figure 12 – MTOM Contour Plot Serial Hybrid with DEP

The resulting MTOM contour plot can be seen in Figure 12. This calculation shows the same basic findings as the one for the serial hybrid without integration benefits. The best MTOM is reached for a split point right above the cruise constraint. For split points below this constraint the MTOM drastically increases and the best point concerning MTOM is not the conventional design point anymore.
The split point with the lowest MTOM is located below the intersection of the climb and new TOD constraint. As can be seen, the cruise power demand decreases further for higher wing loadings but only slightly while the overall power demand strongly increases with the TOD constraint. That makes a higher wing loading not feasible as the savings in fuel and smaller ICE are eaten up by a much heavier EM.
Still, the MTOM decreases in comparison to the hybrid without integration benefits by roughly 12 % and is only approximately 4 % heavier than the conventionally powered aircraft. Concerning primary energy usage and fuel consumption, it is even better than the conventional one. It consumes about 12 % less fuel and about 11 % less primary energy. Even if the overall aircraft is heavier, those savings come from the much lower power demand during cruise for the higher wing loading. Detailed information on the aircraft can be found in Table 7. The Hp,serial of this aircraft would be roughly 1.32, meaning the Range Extender unit is able to deliver about 75 % of the EM power.

With the DEP concept, which includes propellers at the wingtips, the induced drag can be reduced [23]. To simulate such a reduction, while assuming an optimized integration of the propellers into the wing, which offers the possibility of further drag reduction [24], another calculation with a new minimum drag coefficient of 0.025 is executed. This is a reduction by about 17 %.
The best split point of this calculation is located at the same wing loading as without the drag reduction, only the P/W is a little lower, which is due to the drag reduction. What changed significantly is the MTOM. For the first time the serial hybrid is now lighter than the conventionally powered aircraft by approximately 3 %. Concerning fuel mass and primary energy usage the reduction is significant, at nearly 30 %. The detailed mass breakdown can be found in Table 8. The $H_{p,serial}$ of this aircraft would be about 1.5.

Table 7 – Results Serial Hybrid-Electric Aircraft with DEP

Serial Hybrid (DEP)	W/S [N/m²]	P/W [W/kg]	MTOM [kg]	Primary E. [GJ]
	785	77	1137	6.02
Δ to conv.	+60%	-8%	+4%	-11%

Mass breakdown, all values in [kg]

Empty mass (w/o engine)		RE mass	Fuel mass	EM mass	Battery mass
554		111	126	17	29
Δ	+4%	nd	-12%	nd	nd

Table 8 – Results Serial Hybrid Electric Aircraft with DEP and Drag Reduction

Serial Hybrid (DEP + Drag Reduction)	W/S [N/m²]	P/W [W/kg]	MTOM [kg]	Primary E. [GJ]
	785	75	1057	4.86
Δ to conv.	+60%	-11%	-3%	-28%

Mass breakdown, all values in [kg]

Empty mass (w/o engine)		RE mass	Fuel mass	EM mass	Battery mass
517		88	101	16	35
Δ	-3%	nd	-29%	nd	nd

5.1. Battery Energy Density Variation

To see how further technology improvements would influence the weight, a parameter variation study on the battery energy density at pack level is conducted. This is done as battery energy density is often identified as the key technology for electric or hybrid-electric propulsion. It was varied from 250 up to 1500 Wh/kg. The study uses the serial hybrid with the DEP concept and the drag reduction as baseline. The results are presented in Table 9.

Table 9 – Results Battery Energy Density Variation

E* [Wh/kg]	**250**	**300**	**350**	**400**
W/S [N/m²]	760	760	760	880
P/W [W/kg]	74	74	74	87
MTOM [kg]	1060	1042	1030	1019
PE [GJ]	4.92	4.84	4.78	4.51
Fuel [kg]	102	101	100	94
Bat [kg]	33	27	23	26
E* [Wh/kg]	**500**	**750**	**1000**	**1500**
W/S [N/m²]	880	880	880	880
P/W [W/kg]	87	87	87	87
MTOM [kg]	1003	982	972	962
PE [GJ]	4.44	4.35	4.31	4.27
Fuel [kg]	92	90	89	88
Bat [kg]	20	13	10	7

What can be seen from the data, which are also visualized in Figure 13, is that the MTOM decreases with increasing battery energy density, just as one would expected. But the changes are not very significant, as the battery is only a small share of the overall mass. For twice the energy density the MTOM decreases by ca. 5 %. Similar values are achieved for primary energy usage and fuel mass, both with about -10%. Figure 13 also shows that the decrease in MTOM for higher energy densities gets lower and lower, the MTOM seems to converge against one value.
From an energy density of 350 to 400 Wh/kg the design and split point of the optimal design change. For the higher values from 400 Wh/kg up it seems feasible to increase the wing loading slightly. The additionally needed batteries are not that heavy at this battery energy density anymore and their and the EM's weight are lighter than the fuel savings that the higher wing loading enables, therefore the aircraft is lighter.

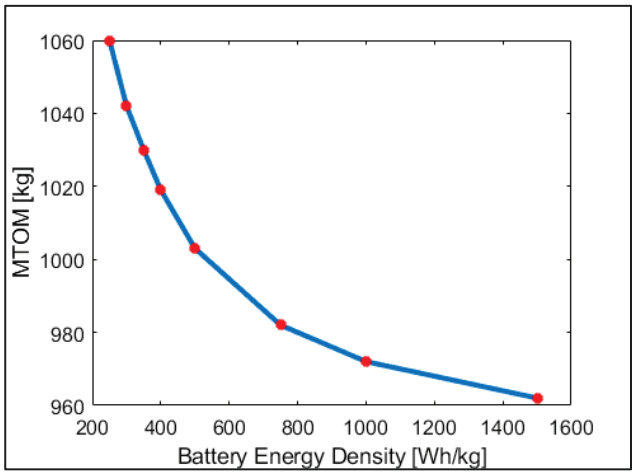

Figure 13 – MTOM over Battery Energy Density

6. CONCLUSION AND OUTLOOK

In this paper the sizing methodology of an initial sizing tool for hybrid aircraft was briefly presented and then used to evaluate light GA aircraft with serial hybrid electric powertrains featuring technology that is already available. Furthermore the influence of several parameters on the design point inside the constraint diagram was analyzed.

A serial hybrid aircraft without relaxing any requirements or using any of the possibilities such a concept offers is about 20 % heavier and uses more fuel than a conventionally powered aircraft. If a distributed electric propulsion concept would be used, which has the potential to increase the maximum lift coefficient as well as the lift coefficient for take-off, a serial hybrid that is only slightly heavier with roughly 4 % more MTOM is possible and would already decrease the fuel mass by 12 %. If this aircraft can also benefit from a reduction of drag, in this study represented by a decrease of about 17 % in C_{D0}, the aircraft would be roughly equal concerning MTOM but use nearly 30 % less fuel. Such fuel savings should make these concepts very interesting for new aircraft designs. An additional study on the effect of battery energy density showed that the savings with improved batteries which are realistic for the near future are not that significant for a serial hybrid aircraft.

Overall, those studies showed that a light serial hybrid aircraft can be viable and should be considered for new aircraft designs as it enables significant fuel savings.
The parameter variation studies on take-off distance, range and cruise velocity that were executed to check their influence on the optimal design point inside the constraint diagram lead to the following results: While the design point was independent from the take-off distance, the other two parameters showed a dependency. For small ranges the conventional design point was better and from a certain range up a split point at the maximum wing loading was best. A similar effect was found for the cruise velocity. A small velocity leads to design and split points at lower wing loadings, while higher velocities favored a design and split point at the maximum wing loading.
As these observations are only valid for this specific set of input parameters and the design point changes also for different hybrids, a new rule for choosing the design point for light serial hybrid aircraft could not be established. But what can be stated is, that the conventional design rule is not valid for light serial hybrid-electric aircraft.

7. REFERENCES

[1] European Commission, Flightpath 2050, Luxembourg: Publications Office of the European Union, 2011.

[2] S. W. Ashcraft, A. S. Padron, K. A. Pascioni and G. W. J. Stout, "Review of Propulsion Technologies for N+3 Subsonic Vehicle Concepts," National Aeronautics and Space Administration, Cleveland, Ohio, 2011.

[3] A. Seitz, A. T. Isikveren and M. Hornung, "Electrically Powered Propulsion: Comparison and Contrast to Gas Turbines," in *61. Deutscher Luft- und Raumfahrtkongress*, Berlin, Germany, 2012.

[4] D. P. Raymer, Aircraft Design: A Conceptual Approach, 5. ed., Reston, Virginia: AIAA, 2012.

[5] M. D. Moore and B. Fredericks, Misconceptions of Electric Propulsion Aircraft and their Emergent Aviation Markets, Virgina: AIAA, 2014.

[6] D. F. Finger, C. Braun and C. Bil, "A Review of Configuration Design for Distributed Propulsion Transitioning VTOL Aircraft," in *Asia-Pacific International Symposium on Aerospace Technology - APISAT2017*, Seoul, Korea, 2017.

[7] A. T. Isikveren, A. Seitz, P. C. Vratny, C. Pornet, K. O. Plötner and M. Hornung, "Conceptual Studies of Universally-Electric Systems Architectures Suitable for Transport Aircraft," in *61. Deutscher Luft- und Raumfahrtkongress DLRK2012*, Berlin, 2012.

[8] C. Pornet, C. Gologan, P. C. Vratny, A. Seitz, O. Schmitz, A. T. Isikveren and M. Hornung, "Methodology for Sizing and Performance Assessment of Hybrid Energy Aircraft," *Journal of Aircraft,* p. 341–352, 2015.

[9] C. A. Perullo, D. Trawick, W. Clifton, J. C. M. Tai and D. N. Mavris, "Development of a Suite of Hybrid Electric Propulsion Modeling Elements using NPSS," in *ASME Turbo Expo*, Düsseldorf, 2014.

[10] D. F. Finger, C. Braun and C. Bil, "Case Studies in Initial Sizing for Hybrid-Electric General Aviation Aircraft," in *2018 AIAA/IEEE Electric Aircraft Technologies Symposium*, Cincinnati, Ohio, 2018.

[11] D. F. Finger, F. Götten, C. Braun and C. Bil, "Initial Sizing for a Family of Hybrid-Electric VTOL General Aviation Aircraft," in *Deutscher Luft- und Raumfahrtkongress 2018*, Friedrichshafen, 2018.

[12] D. F. Finger, C. Braun and C. Bil, "An Initial Sizing Methodology for Hybrid-Electric Light Aircraft," in *2018 Aviation Technology, Integration, and Operations Conference*, Atlanta, Georgia, 2018.

[13] S. Gudmundsson, General Aviation Aircraft Design: Applied Methods and Procedures, Boston: Elsevier, 2014.

[14] R. Gagg and E. Farrar, Altitude Performance of Aircraft Engines Equipped with Gear-Driven Superchargers, Michigan: SAE Technical Paper 340096, 1934.

[15] Wissenschaftliche Dienste Deutscher Bundestag, Sachstand: Primärenergiefaktoren, Berlin: Deutscher Bundestag, 2017.

[16] "Cessna Textron Aviation Skyhawk Specs," [Online]. Available: cessna.txtav.com/en/piston/cessna-skyhawk#_model-specs. [Accessed 29 January 2018].

[17] R. Rings, J. Ludowicy, D. F. Finger and C. Braun, "Sizing Studies of Light Aircraft with Parallel Hybrid Propulsion Systems," in *Deutscher Luft- und Raumfahrtkongress 2018*, Friedrichshafen, 2018.

[18] E. Torenbeek, Advanced Aircraft Design, John Wiley & Sons, 2013.

[19] R. Rings, Preliminary Sizing Studies of Light Aircraft with Parallel Hybrid Propulsion Systems, Aachen: FH Aachen, 2018.

[20] National Aeronautics and Space Administration, "NASA Armstrong Fact Sheet: NASA X-57 Maxwell," [Online]. Available: www.nasa.gov/centers/armstrong/news/FactSheets/FS-109.html. [Accessed 20 August 2018].

[21] J. K. Viken, S. A. Viken, K. A. Deere and M. B. Carter, "Design of the Cruise and Flap Airfoil for the X-57 Maxwell," in *35th AIAA Applied Aerodynamics Conference*, Denver, Colorado, 2017.

[22] M. D. Moore, "Distributed Electric Propulsion (DEP) Aircraft," [Online]. Available: aero.larc.nasa.gov/files/2012/11/Distributed-Electric-Propulsion-Aircraft.pdf. [Accessed 20 August 2018].

[23] J. M. H. Snyder and G. W. Zumwalt, "Effects of Wingtip-Mounted Propellers on Wing Lift and," *Journal of Aircraft,* pp. 392-397, 09 1969.

[24] H. Epema, "Wing Optimisation for Tractor Propeller Configurations," Delft University of Technology, 2017.